MULTIDIMENSIONAL MODELLING OF THE IN-CYLINDER PROCESSES IN A GDI ENGINE

A. Montanaro[(a)], U. Sorge[(b)], F. Catapano[(c)],B.M. Vaglieco[(d)]

[(a), (d)]CNR – Istituto Motori, Viale Marconi, 8 – 80125, Naples, ITALY
[(b), (c)]DIME – University of Naples, Via Claudio, 21 – 80125, Naples, ITALY

[(a)]a.montanaro@im.cnr.it, [(b)]u.sorge@im.cnr.it, [(c)]f.catapano@im.cnr.it, [(d)]b.m.vaglieco@im.cnr.it

ABSTRACT
The study is focused on the assessment of a 3D numerical model able to simulate the in-cylinder processes characterizing the operation of GDI (gasoline direct injection) engine equipped with a high-pressure injector system. The engine is experimentally characterized at the test bench. One of the 4 cylinders is modified to allow two optical accesses that leave unvaried the combustion chamber configuration and allows capturing images of the mixture formation and combustion processes. A sub-model of high portability allows simulating the spray dynamics, whose validation is made on the ground of experimental data collected with the injector mounted in a confined vessel. A preliminary study of the spray-wall impingement is also carried out, that allows better predicting the gasoline deposition and splashing phenomena.

Keywords: multidimensional engine modeling, gasoline direct injection, spray-wall impingement

1. INTRODUCTION

A way to significantly improve the energetic efficiency of internal combustion engines without making a major shift away from conventional technologies is well recognized in the use of direct injection (DI). In spark ignition (SI) engines, in particular, gasoline direct injection (GDI) is today considered indispensable to decrease fuel consumption, hence CO_2 emissions, as coupled with downsizing and turbo-charging. Thanks to the more precise control of the injection timings feasible through DI, well known limits of the port fuel injection (PFI) engines in the combustion control and fuel supply response are overwhelmed. The GDI technology, indeed, especially with the employment of new generation high-pressure injectors in the multi-hole configuration, has the great advantages of improving the mixture formation process, with a positive effect on combustion stability and pollutant emissions formation. Knock tendency is also favorably affected due to the decrease of the charge temperature consequent the in-cylinder gasoline evaporation [Alkidas, 2008]. Nevertheless, the complexity of modern engines makes for assuring optimal mixture conditions at all the engine loads and speeds to be a really difficult task. Exploiting the capability of numerical techniques to achieve a complete control of the mixture formation process over the whole engine working map, to increase fuel economy, improve combustion stability, and reduce engine-out emissions is surely an issue of great importance in the automotive field.

Present work is aimed at developing a 3D engine model of the in-cylinder processes occurring in a modern GDI engine. The engine model assessment is supported by three experimental campaigns. The employed seven-hole injector is first preliminary experimentally characterized in a confined vessel and on a Bosch tube to tune the 3D sub-model for the spray dynamics. Experiments relevant to collect data for the validation of the sub-model for the spray-wall impingement are also carried out by making for the spray to orthogonally hit a flat plate, possibly heated at some given temperatures. Finally the engine is characterized to collect in-cylinder pressure data and images of the spray development. The engine, in fact, exhibits optical accesses enabling to explore an area including the spark and the gasoline spray. After a short description of the sub-models assessment, main results of the 3D engine simulation are presented, with reference to an overall lean, medium-speed medium-load operating condition.

2. EXPERIMENTAL APPARATUS

2.1. Spray Characterization

The GDI injector considered in the present work is a mini-sac seven-hole Bosch HDEV 5.1 with solenoid actuation. The injector holes diameter is equal to 0.179 mm. The static flow rate is of 13.7 g/s at the injection pressure of 10 MPa. Figure 1 represents a sketch of the spray footprint, drawn on a plane orthogonal to the injector axis, placed at a distance of 30 mm from the holes.

Commercial gasoline (ρ = 740 kg/m3) is used within all the experimental campaign, as delivered by a hydro-pneumatic injection system without rotating organs. The injector system is managed by a programmable electronic control unit (PECU). This is an open system able to reproduce the injector energizing currents for the desired strategy in terms of number of injection pulses, durations, rise and dwell times. The

PECU reproduces as an output a TTL signal, related to the injection event, used to synchronize also the consecutive images management and acquisitions. The PECU, in fact, also control the synchronized image acquisition set-up.

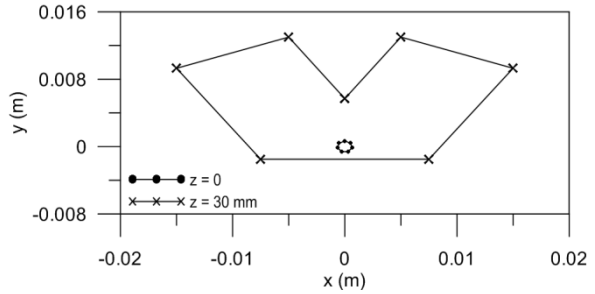

Figure 1: Holes position and spray footprint on a plane placed at 30 mm form the holes.

Three types of analysis are conducted: a) instantaneous mass flow rates are measured by means of an AVL Meter operating on the Bosch principle [Bosch, 1996; Wallace, 2002]; b) the single jet penetration length and cone angle of a freely developing spray are obtained by image processing techniques; c) the spray impingement on an orthogonal wall, possibly heated by image processing is used to characterize.

The instantaneous mass flow rate measured by the AVL fuel rate meter is integrated to gain the total injected mass and to verify its accordance with the measured one by means of a precision balance.

Images of the spray are collected by injecting the spray in an optically-accessible vessel containing nitrogen at controlled conditions of temperature and pressure. The injector command is generated by the PECU. A synchronized pulse starts both the flash enlightening and shutter of a high-resolution CCD camera (1376x1040 pixels, 12 bit resolution, 0.5 μs shutter time). Images of the spray are collected at different instants from the start of injection (SOI) with a 50 mm lens obtaining a spatial resolution 0.103 mm/pixel (while for impinging test at 0.0658 mm/pixel). An overview of the experimental scheme for the image acquisition is reported in [Alfuso., Allocca, Greco, Montanaro, Valentino, 2008]. The captured images are processed off-line by means of a proper software, able to extract the parameters characterizing the spray dynamics, namely penetration length and cone angle of one of the seven jets compounding the spray. The images processing analysis is carried out in different steps: image acquisition and background subtraction, filtering, fuel spray edges determination and tip penetration measurements. Background subtraction and median filter procedures are adopted during the image acquisition to remove impulse noise and stray light, so to maintain sharp the spray edge. This is determined by selecting an intensity threshold level for separating the fuel region from the background ambient gas. The experiments devoted to determine the spray atomization characteristics in the case of impingent on an orthogonal wall are carried at different injection pressures (p_{inj}), wall distance (h) and wall temperature (T_{wall}). Two of the considered conditions are reported in Table 1.

p_{inj} (MPa)	5.5	5.5
T_{wall} (K)	300	473.15
h (mm)	20	20

Table I: Experimental conditions for impinging sprays.

2.2. Optical Engine

The experimental apparatus for the characterisation of the engine performance includes the following modules: the spark ignition engine, an electrical dynamometer, the fuel injection line, the data acquisition and control units, as well as the emission measurement system. The electrical dynamometer allows the engine operation under both motored and firing conditions.

The engine under study is a SI DI, inline 4-cylinder, 4-stroke, displacement of 1750 cm^3, turbocharged, high performance engine. It has a wall guided injection system with a seven-hole injector located between the intake valves and oriented at 70° with respect to the cylinder axis. The engine is equipped with a variable valve timing (VVT) system in order to optimize intake and exhaust valve lift for each regime of operation. The engine is not equipped with after-treatment devices. Further details of the engine are reported in Table II.

Unitary displacement [cm^3]	435.5
Bore [mm]	83
Stroke [mm]	80.5
Turbine	Exh. gas turbocharger
Max. boost pressure [bar]	2.5
Valve timing	Intake and exhaust VVT
Compression ratio	9.5:1
Max. power [kW]	147.1 @ 5000 rpm
Max. torque [Nm]	320.4 @ 1400 rpm

Table II. Engine specifications

Optical measurements are carried out through an optical access on the engine head, as reported in Figure 2. A custom protective case for an endoscopic probe, equipped with an optical sapphire window (5 mm in diameter), is installed in the engine head in the 4th cylinder. This system enables exploring an area including the spark and the fuel injection using an endoscope with a viewing angle of 70°. The field of view turns out to be centered in the combustion chamber and perpendicular to the plane of tumble motion.

Imaging measurements from ultraviolet (UV) to visible are performed by means of the optical experimental set-up shown in Figure 2. In particular, the endoscopic probe is coupled to a high spatial and temporal resolution intensified charge coupled device (ICCD) camera. It has a 78 mm focal length, f/3.8 UV Nikon objective, and an array size of 512x512 pixels and 16-bit dynamic range digitization at 100 kHz. The

optical assessment allows a spatial resolution approximately 0.19 mm/pixel, and a spectral range from UV (180 nm) until visible (700 nm). The intensifier-gate duration is equal to 1° crank angle (CA) for all investigated conditions. The dwell time between two consecutive images is set at 1° CA. A post-processing of the optical data is applied to obtain geometrical information from each image, such as the flame front area and the radius [Sementa, Vaglieco, Catapano, 2012]. Moreover, a quartz pressure transducer is installed into the spark plug in order to measure the combustion pressure. The in-cylinder pressure and the related parameters as the coefficient of variance (COV) of the IMEP, and the rate of chemical energy release are evaluated on an individual cycle basis averaged over 500 cycles [Heywood, 1988; Zhao, Ladommatos, 2001].

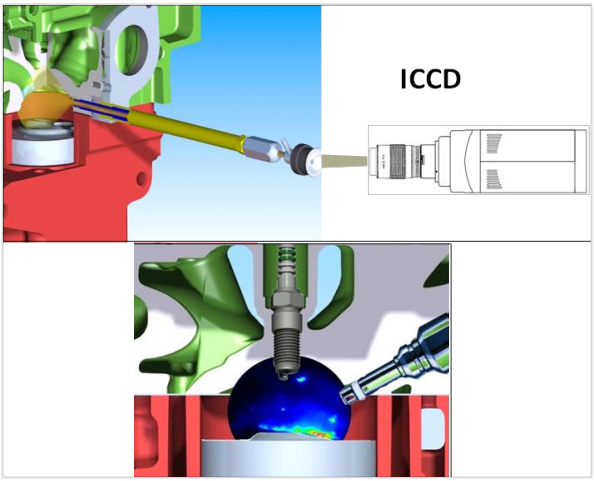

Figure 2: Sketch of the experimental setup for optical investigation and detail of the combustion chamber

The engine test discussed in the following of the paper is that relevant to an engine speed of 1500 rpm, a medium load (injected gasoline m_f= 20.16 mg/cycle, air to fuel ratio A/F= 16.9), injection pressure of 6 MPa, start of spark (SOS) set at 13° before the top dead center (BTDC) and start of injection (SOI) at 70° BTDC.

3. NUMERICAL SIMULATION

The here discussed 3D engine model is developed within the software AVL Fire™. The preliminary phase of the model set-up consisted in the assessment and validation of the sub-models for the spray dynamics and of the spray wall impingement, made by reproducing the experimental tests described in section 2.1. These aspects, indeed are believed of great importance to well reproduce the mixture formation process in a GDI engine.

The approach followed for the description of the two-phase turbulent flow is the classical coupling between the Eulerian description of the gaseous phase and the Lagrangian description of liquid phase. The coupling between the two phases is made through source terms representing the exchange of mass, momentum and energy in the balance equations.

3.1. The sub-models for the spray dynamics and the wall impingement

The spray is assumed as a train of droplets entering the computational domain at the initial time and with a given distribution of diameters. The effects of turbulent dispersion, coalescence, evaporation, wall interaction and break-up of droplets are treated with proper sub-models. In particular, the effect of the turbulent dispersion is treated following the sub-model by O'Rouke [O'Rourke, Bracco., 1980], coalescence with the sub-model by Nordin [Nordin, 2001], evaporation with the sub-model by Dukowicz [Dukowicz, 1979]. The model used to reproduce the wall interaction is the one proposed by Kuhke [AVL Fire™ User Guide, 2011].

Details of the validation phase of the sub-model reproducing the dynamics of a freely developing non evaporating spray are given in the paper by Costa *et al.* [Costa, Sorge, Allocca, 2012]. Some results are here reported.

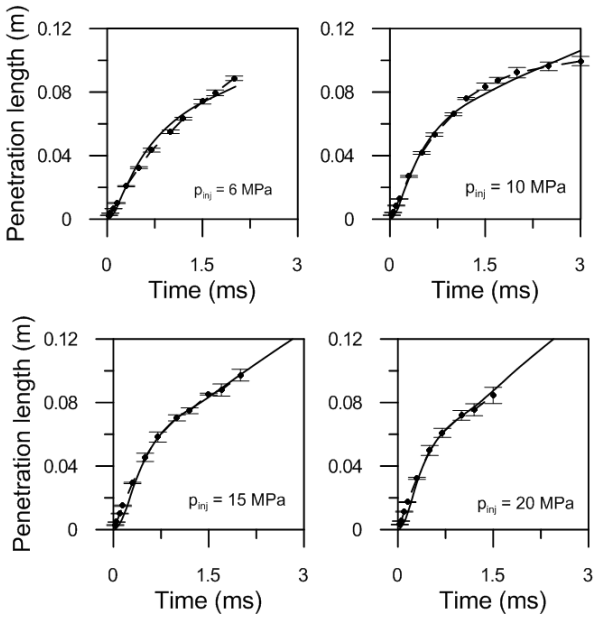

Figure 3: Numerical (continuous line) and experimental (dashed line with dots) penetration lengths of the GDI spray in confined vessel at various pressures. Error bars are also represented.

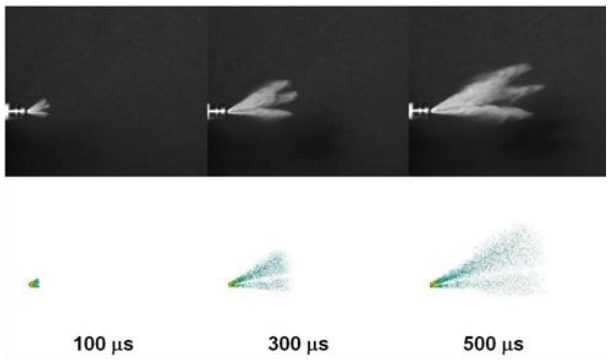

Figure 4: Experimental collected (top) and numerical computed (bottom) images of the spray at the injection pressure of 15 MPa

Figure 3 is the comparison between the numerical (average over the seven jets) and the experimentally measured penetration lengths (one of the seven jets) for four different injection pressures. The agreement between the sub-model results and the experiments is really good. The spray structure is also quite well reproduced, as shown in Figure 4, that shows experimental and numerical images of the spray at various instants of time from the SOI at p_{inj}=15 MPa.

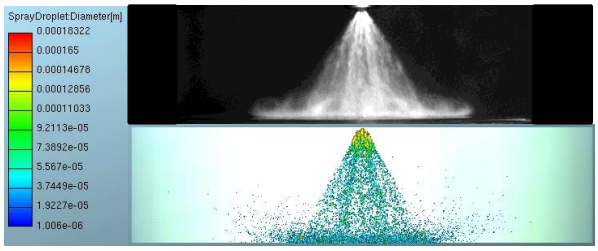

900 μs after SOI

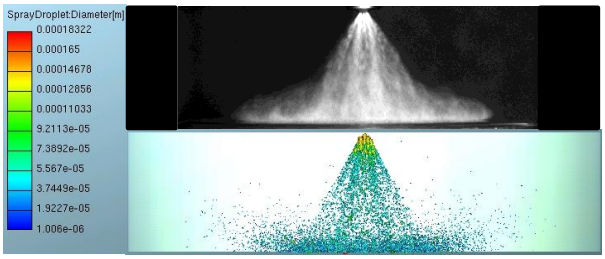

1100 μs after SOI

Figure 5: Comparison between experimental (top) and numerical (bottom) images of impinging sprays for p_{inj}= 5.5 MPa, T_{wall} = 300 K at two instants of time.

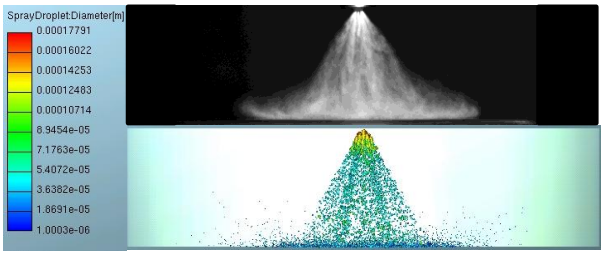

900 μs after SOI

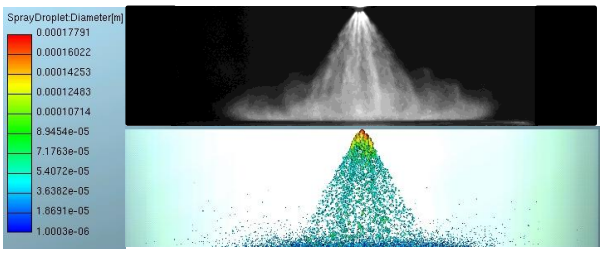

1100 μs after SOI

Figure 6: Comparison between experimental (top) and numerical (bottom) images of impinging sprays for p_{inj}= 5.5 MPa, T_{wall} = 473 K at two instants of time.

The impingement of a spray on a wall gives rise to the deposition of a liquid film and to a secondary atomization of the impacting droplets. The process is strongly affected by the conditions of pressure, velocity and temperature of the surrounding gas and by the value of the wall temperature. The tuning of the impingement sub-model is here carried out at different injection pressures, initially for T_{wall}= 300 K, than by considering impingement on a warm wall (T_{wall} = 473 K).

The spray structure of the wall impingement process is shown in Figure 5. The comparison between the experimental measurement s and the numerically computed spray is made at 900 μs and 1100 μs after the SOI, for T_{wall} = 300 K, p_{inj} = 5.5 MPa, h= 20mm. The comparison relevant to T_{wall} = 473 K, are reported in Figure 6, again at 900 and 1100 μs after SOI. The numerical computation well describes the shape and the impingement of the spray, for both the examined cases.

3.2. The 3D Engine Model

The discretization of the computational domain is made through a home-made procedure, instead than resorting just to the pre-processing software included in the AVL Fire™ graphical user interface (GUI), namely the fame engine plus (FEP) module.

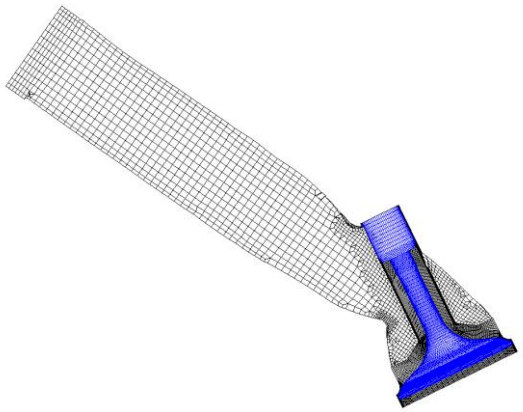

Figure 7: Computational grid relevant to the intake duct.

The search for a compromise solution between accuracy of results and low calculation time, indeed, needs a "customized" methodology for the grid design, able to allow easy changes as a consequence of possible variations of the valve lift profile. The computational domain made of the cylinder and the intake and exhaust ducts is subdivided into different sub-domains, some of which are discretized through the FEP module, while others are discretized "manually", to only generate hexahedral cells. Figure 7, as an example, shows the volume surrounding the intake valve and the intake duct. The cells are all hexahedral around the valve, as obtained by rotation of a regular 2D properly designed grid. Finally, Table III is indicative of the employed cell numbers. It is to be pointed out that different ranges are considered, namely different intervals of crank angles are taken, with domain activated or deactivated depending on the particular stroke being considered (in the closed valves period, say, the computational domain is made of just the combustion chamber - the intake duct is activated and really attached to the combustion chamber only when intake valves starts being opened).

Also, data reported in Table III are mean ones, namely indicative numbers typical of the grid size used in a certain range. In the Fire code, in fact, a "rezone" is necessary to avoid excessive cells distortion, hence the grids are substituted by other ones when the cell quality gets worst.

Range	Cells number
Exhaust Stroke	390000
Intake Stroke	331000
Closed Valve Period	185000

Table III: Employed grid resolution.

The charge turbulent motion within the computational domain is modeled through the k-ζ-f model, the combustion process according to the ECFM 3Z model [Colin, Benkenida, Angelberger, 2003]. NO formation follows the extended mechanism formulated by Zeldovich. A semi-empirical model for soot formation is also considered. Boundary conditions for the 3D model are derived from experimental measurement in the intake and exhaust ducts. Initial conditions are set according to the experimental data. The computation is initiated at the crank angle of top dead center (TDC), some degrees before the intake valves opening (IVO).

The whole engine cycle is simulated. A preliminary validation phase, here not reported for the sake of brevity regarded the computation of a motored pressure cycle, the check about the repeatability of results obtained over more than one computational cycle (necessary due to the kind of imposed initial conditions) and a check about the grid invariance of the obtained results. The comparison between the experimentally measured and the numerically computed pressure cycle in the medium-speed, medium-load lean condition is reported in Figure 8. Both the intake stroke and the compression stroke are quite well reproduced. The combustion phase is also in good agreement.

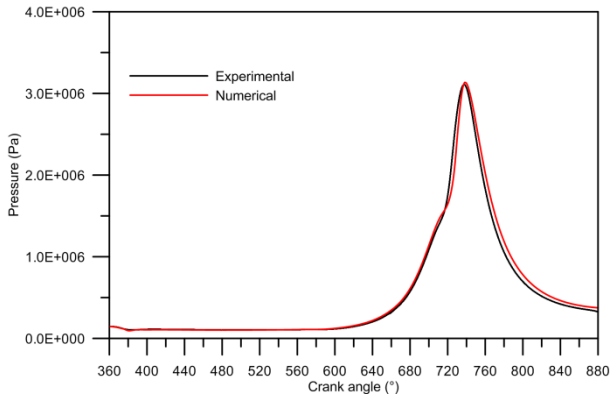

Figure 8: Comparison between the experimental collected and numerically computed pressure cycles.

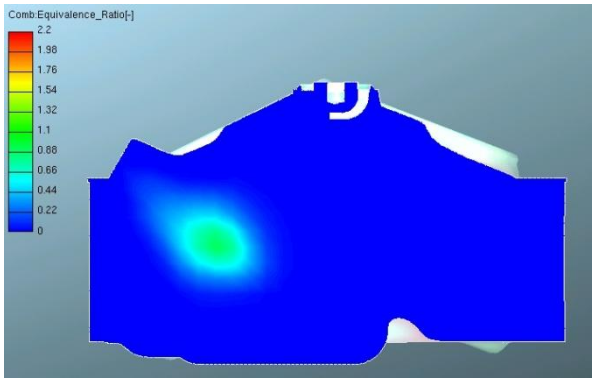

6° after SOI.

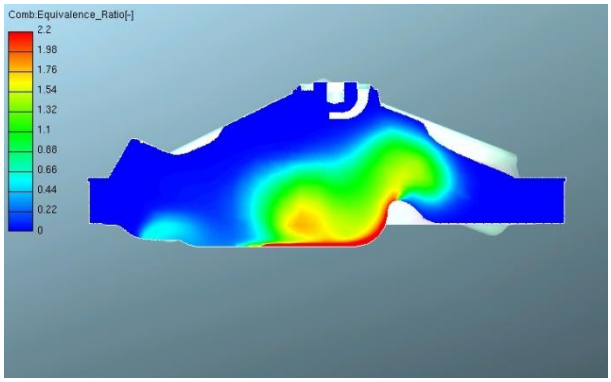

40° after SOI.

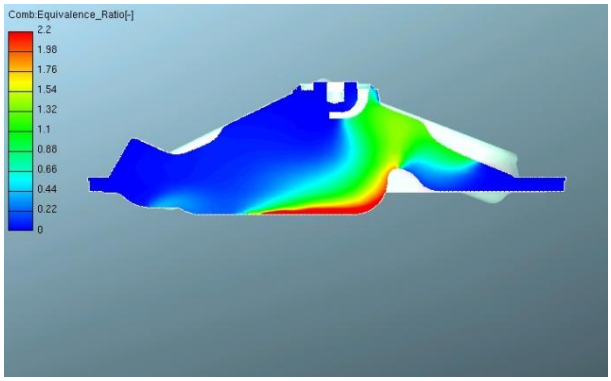

SOS

Figure 9: Numerical equivalence ratio distribution on a plane passing through the spark plug at various crank angles after SOI.

The reliability of the assessed model in reproducing the in-cylinder processes is good. Detailed information concerning the mixture formation and combustion evolution, therefore, can be derived by drawing relevant variables distributions on some internal planes. Figure 9, as an example, shows the distribution of the mixture equivalence ratio (local air to fuel ratio over stoichiometric air to fuel ratio) on a plane passing through the spark plug at three different instants of time, namely 6° after SOI, 40° after SOI and at the time of spark ignition (SOS).

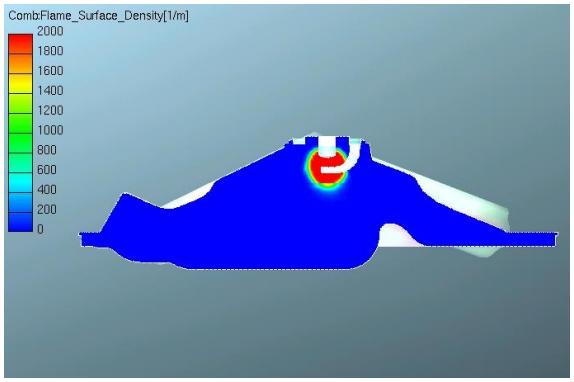

SOS.

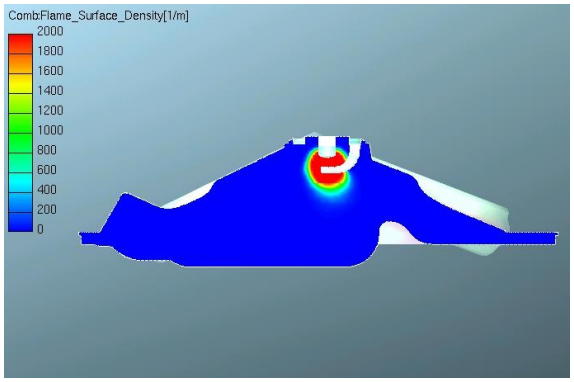

2° after SOS (TDC).

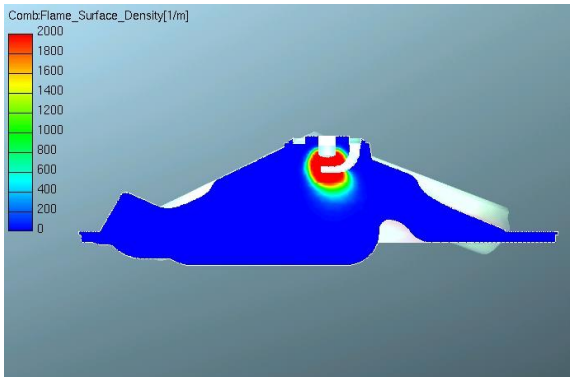

3° after SOS.

Figure 10: Flame surface density distribution on a plane passing through the spark plug at various crank angles after SOS.

The flame front evolution after SOS is instead shown in Figure 10.

4. CONCLUSIONS

Experiments performed to characterize the dynamics of a freely evolving spray issuing from a seven-hole injector and its impingement on a cold or heated wall are used to tune proper sub-models to be included in a 3D engine model. This last is assessed to reproduce the in-cylinder phenomena of a high performance GDI engine, also experimentally characterized at the test bench. The presented model is suitable of being included within a multi-objective optimization tool to optimize the engine performance, by changing input parameter as injection strategy or time of spark ignition.

REFERENCES

Alkidas, A.C., 2007,Combustion Advancements in Gasoline Engines, *Energy Conversion and Management* 48; 2751-2761.

Bosch, W., 1966, The fuel rate indicator: a new measuring instrument for display of the characteristics of individual injection, SAE Paper 6607496.

Wallace, I., 2002, Injection Rate Gauge: Pass Off Information and User Instruction, *Fuel & Engine Management System*, Graz.

Alfuso, S., Allocca, L., Greco, M., Montanaro, A., Valentino, G., 2008, Time and Space Characterization of Multi-hole GDI Sprays for IC Engines by Images Processing and PDA Techniques, ILASS08-071.

Sementa, P., Vaglieco, B.M., Catapano, F., 2012, Thermodynamic and optical characterizations of a high performance GDI engine operating in homogeneous and stratified charge mixture conditions fueled with gasoline and bio-ethanol, *Fuel*, 96, 204 – 219.

Heywood, J.B., 1988, *Internal Combustion Engine Fundamentals*, New York: McGraw-Hill.

Zhao, H., Ladommatos, N., 2001, *Engine Combustion Instrumentation and Diagnostics*. SAE Int., Inc.

O'Rourke, P.J., Bracco, F.V., 1980, Modeling of Drop Interactions in Thick Sprays and a Comparison with Experiments, *Institution of Mechanical Engineers (IMECHE)*, London.

Nordin, W.H., 2001, *Complex Modeling of Diesel Spray Combustion*, Thesis (PhD), Chalmers University of Technology.

Dukowicz, J.K., 1979, Quasi-steady droplet change in the presence of convection, informal report Los Alamos Scientific Laboratory, *Los Alamos Report LA7997-MS*.

AVL Fire™ v2011 User Guide – Lagrangian - Multiphase.

Costa, M., Sorge U., Allocca L., 2012, CFD Optimization for GDI Spray Model Tuning and Enhancement of Engine Performance, *Advances in Engineering Software*, 49, 43 – 53.

Colin, O., Benkenida, A., Angelberger, C., 2003, 3D Modeling of Mixing, Ignition and Combustion Phenomena in Highly Stratified Gasoline Engines, *Oil & Gas Sciense and Technology – Rev. IFP Energies Nouvelles*, 58 47-62.